



This is the accepted manuscript made available via CHORUS. The article has been published as:

Criteria for Erroneous Substrate Contribution to the Thermoelectric Performance of Thin Films

A. Riss, M. Stöger, M. Parzer, F. Garmroudi, N. Reumann, B. Hinterleitner, T. Mori, and E. Bauer

Phys. Rev. Applied **19**, 054024 — Published 8 May 2023

DOI: [10.1103/PhysRevApplied.19.054024](https://doi.org/10.1103/PhysRevApplied.19.054024)

Criteria for erroneous substrate contribution in thermoelectric thin films

A. Riss,^{1,*} M. Stöger,¹ M. Parzer,¹ F. Garmroudi,¹ N. Reumann,¹ B. Hinterleitner,¹ T. Mori,^{2,3} and E. Bauer¹

¹*Institute of Solid State Physics, Technische Universität Wien, 1040 Vienna, Austria*

²*International Center for Materials Nanoarchitectonics (WPI-MANA),*

National Institute for Materials Science, Tsukuba 305-0044, Japan

³*University of Tsukuba, Tsukuba 305-8577, Japan*

Thermoelectric materials have attracted considerable interest for energy applications such as waste-heat recovery and energy harvesting to power Internet-of-Things sensors. In the past decades, an increasing number of different strategies to increase the performance have been invented and tested, including the synthesis of thin films and other high performance multi-layered structures. Although it has already been shown that the pure combination of the properties of each layer without interactions will yield a worse performance compared to the best layer, a critical estimation of the size of the deviation to trace back the single properties is still missing. In this paper, we derive a set of formulas to describe the total Seebeck coefficient, electrical and thermal conductivity, power factor and zT value of a two-layer system from a simple model and elucidate the origin and size of the contribution of each layer to the total thermoelectric performance. We further show that the influence of the substrate can lead to large deviation between the measured and the film's properties, advising caution when analysing such systems. Moreover, this model allows to ensure the contribution of the substrate to be lower than a desired threshold by introducing material-related quantities $\varepsilon_{\sigma,\lambda}$.

I. INTRODUCTION

Increasing the efficiency of energy utilization is an important task regarding the progression of the global climate and energy crisis. Estimations by Forman *et al.* revealed that the majority of the global primary energy ($\approx 72\%$) is lost at conversion, with thermal losses having the largest share [1]. In addition, energy harvesting for Internet-of-Things (IoT) sensors has recently become an important topic [2, 3]. One promising power source for these sensors are thermoelectric devices, which have the ability to directly convert waste heat into electricity by making use of the Seebeck effect. The performance of such a device is described by its dimensionless figure of merit $zT = (S^2\sigma/\lambda)T$, where T is the absolute temperature, S the Seebeck coefficient, σ the electrical conductivity and $\lambda = \lambda_{\text{ph}} + \lambda_{\text{e}}$ the total thermal conductivity, consisting of the phononic part λ_{ph} and the electronic part λ_{e} . For substantial waste-heat harvesting, zT should exceed 1.5 [4].

Despite the clear-looking path to obtain a high efficiency, *i.e.* maximizing the Seebeck coefficient and the electrical conductivity and minimizing the thermal conductivity, the fact that all electronic quantities strongly depend on the charge carrier density makes a simultaneous enhancement of all difficult. The phononic part of the thermal conductivity on the other hand can often independently be tuned, which is why huge effort is put in increasing the thermoelectric performance via reduction of the lattice contribution λ_{ph} with remarkable success for example by thin film deposition [5–15].

Beside this reduction of the thermal conductivity, even enhancements of the power factor $S^2\sigma$ were found in thin

two-layer systems in recent years [16–22]. Clarifying the individual contributions of the substrate to the overall thermoelectric performance is essential in accurately assessing a film's properties. This is particularly relevant in cases where the power factor improves with decreasing film thickness, as observed in various research studies.

Yordanov *et al.* reported a significantly enhanced Seebeck coefficient in $\text{Ca}_3\text{Co}_4\text{O}_9$ thin films on SrTiO_3 and LaAlO_3 substrates, compared to the bulklike values obtained on $[\text{LaAlO}_3]_{0.3}-[\text{Sr}_2\text{AlTaO}_6]_{0.7}$, LaSrAlO_4 and MgO substrates [16]. They attributed the enhancement of the total Seebeck coefficient S_{t} to the contributions of the substrate and the interface layer using the well-known formula

$$S_{\text{t}} = \frac{\sum_i S_i \sigma_i d_i}{\sum_i \sigma_i d_i}, \quad (1)$$

where σ_i is the electrical conductivity, d_i the thickness and $i = \{\text{film, int, sub}\}$ denotes the film, the interface layer and the substrate, respectively. Under the assumption that the electric current only flows through the film, the electrical conductivity was calculated, revealing a power factor above 1.5 mW/mK^2 on SrTiO_3 at 993 K.

Shimizu *et al.* found an enhancement of the Seebeck coefficient from $+3.8 \mu\text{V/K}$ to $-454 \mu\text{V/K}$ at 200 K in FeSe films on SrTiO_3 by reducing the thickness to 1 nm [17]. The authors contributed this increase to a transition of the density of states from a 3D to a 2D behavior and ruled out any influence of the substrate due to the screening nature of the metallic film as well as the formation of a Schottky barrier between the layers. Together with a small resistivity, calculated using only the film's thickness, they achieved a record-high power factor of 1300 mW/mK^2 at 50 K and 26 mW/mK^2 at room temperature.

* alexander.riss@tuwien.ac.at

Zhang *et al.* reported a power factor of 1.78 mW/mK^2 at 700 K in MoO_{2+x} films on a Si substrate, being around 42 times larger than the value obtained from the same film on a quartz substrate [18]. Subsequently, a further increase of the power factor of up to 12.5 mW/mK^2 at 668 K was reported by reducing the thickness of the film from 700 nm to 130 nm [22].

Apart from film-substrate systems, Byeon *et al.* found extreme values of the figure of merit $zT \approx 471$ in Cu_2Se , when a large vertical temperature gradient was applied, in addition to the horizontal one used to measure the thermovoltage [19, 20]. The vertical temperature difference inside the material ($\approx 40 \text{ K}$) causes a structural phase transition at the hotter side. The authors concluded that both an extraordinary large Seebeck coefficient associated with the low-temperature phase, as well as the low electrical resistivity of the high-temperature phase are measured simultaneously, leading to a very high power factor. A large value of $zT \approx 20$ was also found in Ag_2S by the same group under the same conditions and interpreted in a similar manner [21].

Contrary to that, Bergman *et al.* mathematically derived that the total power factor and figure of merit of a 2-material composite are worse than those of the better material when property-changing interactions are neglected [23, 24]. Furthermore, Alvarez-Quintana obtained a reduction of the thermoelectric figure of merit for a parallel setup of a film-substrate system due to heat and current flow through the latter. The degree of reduction was found to be dependent on the ratio of the thickness of the substrate to the thickness of the film [25].

In this work, we investigate the thermoelectric behavior of multi-layer systems from a theoretical point of view and highlight the importance of critical analysis of the measurement data in more complex systems. By doing so, we make no statement about effects such as diffusion, energy filtering, confinement, lattice distortion, epitaxial growth, charge transfer or others, which can additionally modify the layer's properties and may contribute to some of the cases reported above. Our calculations will only focus on the total performance due to the interplay of the single properties of each layer.

II. ANALYSIS OF THE THERMOELECTRIC PROPERTIES OF A FILM-SUBSTRATE SYSTEM

When a temperature gradient is applied along the surface of a film, all layers, including the substrate, are affected as well. In order to allow for a proper evaluation of the performance, all individual quantities and potential contributions need to be considered. Each layer of a multi-layer system comprises of electrical and thermal resistances, and a voltage that is proportional to the material's Seebeck coefficient. For the purpose of calculating the overall Seebeck coefficient and electrical conductivity, the system can be modelled by an electric circuit with voltage sources and internal electrical resistances.

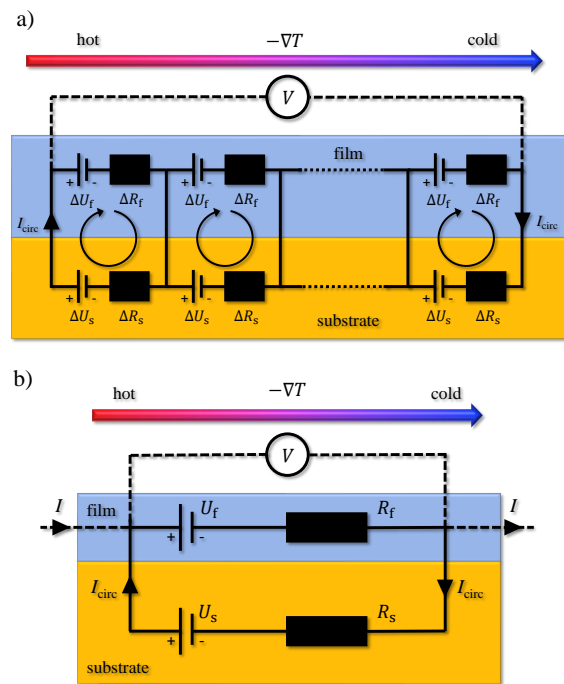


Figure 1: a) Electric circuit modelling the film-substrate system without an interface layer. Each layer consists of a voltage source $U_i = \sum \Delta U_i$ and an electrical resistance $R_i = \sum \Delta R_i$ ($i = \{\text{film, substrate}\}$). The voltage difference leads to circular currents I_{circ} , altering the measured Seebeck coefficient. b) Simplified model without the inner connections between film and substrate. The resistance is measured by applying an external current I .

A common scenario of this type is a film deposited on a substrate, as shown in Figure 1a. To focus on the contribution of the substrate, the model neglects a potential interface layer between film and substrate and effects altering the properties of either layer, although they can be considered within the individual quantities.

The interface connections divide the circuit into smaller sub-circuits. The sub-voltages cause circular currents flowing through the surface and the nearest interface connection, as alternative paths have a higher resistance. As a result, opposing interface currents from neighboring circuits cancel out each other, leading to the net current I_{circ} only flowing through the edge of the interface. To fully describe the system it is therefore sufficient to only connect the layers on both ends, as shown in Figure 1b.

When measuring resistance and thermovoltage, film and substrate form a parallel system. Without considering the chemical interaction at the interface, the total resistance R_t can thus be written as

$$R_t = \frac{R_f R_s}{R_f + R_s}, \quad (2)$$

with $R_{f,s}$ being the resistance of the film and the substrate, respectively. R_f is therefore calculated as

$$R_f = (1 + \varepsilon_\sigma) R_t, \quad \text{with} \quad \varepsilon_\sigma := \frac{R_t}{R_s - R_t} = \frac{R_f}{R_s}. \quad (3)$$

ε_σ describes the ratio of the resistance of the film to the substrate resistance and determines the influence of the substrate on the total Seebeck coefficient and electrical conductivity of the system, as we show below.

Unlike the resistance, the thermovoltage is measured in open-circuit conditions. In order to understand the effect of the combined layers on the Seebeck coefficient, a modification of the entire thermovoltage due to the short-circuiting of the two materials needs to be taken into consideration. The circular current arising in the film-substrate system when a temperature gradient is present along the surface changes the measured thermovoltage due to the potential drop at the resistor. By applying Kirchhoff's law, the value of the current is obtained:

$$I_{\text{circ}} = \frac{U_s - U_f}{R_f + R_s}. \quad (4)$$

Thus, the measured voltage and Seebeck coefficient can be calculated using

$$\begin{aligned} U_t &= U_f + IR_f \\ &= \frac{U_f R_s + U_s R_f}{R_s + R_f} \end{aligned} \quad (5)$$

and

$$S_t = \frac{S_f R_s + S_s R_f}{R_s + R_f}, \quad (6)$$

where $U_{f,s}$ and $S_{f,s}$ are the voltage and the Seebeck coefficient of the film and the substrate, respectively. As film and substrate usually have the same surface dimensions, Equation 6 can be rewritten in accordance to Equation 1 as

$$S_t = \frac{S_f \sigma_f d_f + S_s \sigma_s d_s}{\sigma_f d_f + \sigma_s d_s}, \quad (7)$$

with the electrical conductivity $\sigma_{f,s}$ and the thickness $d_{f,s}$ of the film and the substrate, respectively. For a multi-layer system the setup can be modified by adding additional voltage sources with internal resistances. This yields the more general expression for the total Seebeck coefficient of a system with i layers

$$S_t = \frac{\sum_i S_i G_i}{\sum_i G_i}, \quad (8)$$

with i denoting the different layers and $G_i = 1/R_i$ being the electrical conductance. For equal surface dimensions of every layer, the equation above simplifies to Equation 1. This formula is frequently used to calculate the influence of the substrate and/or interface layer on the

total Seebeck coefficient.

Inserting Equation 3 into Equation 6 gives the total Seebeck coefficient of a two-layer system in dependence of our newly defined weighting parameter ε_σ :

$$S_t(\varepsilon_\sigma) = \frac{S_f + \varepsilon_\sigma S_s}{1 + \varepsilon_\sigma}. \quad (9)$$

Considering this formula, the contribution of the substrate only depends on the parameter ε_σ and the total Seebeck coefficient has the following limits:

$$S_t = \begin{cases} S_f & \text{for } \varepsilon_\sigma = 0 \\ S_s & \text{for } \varepsilon_\sigma \rightarrow \infty \end{cases}. \quad (10)$$

For all other values of ε_σ the total Seebeck coefficient lies between those of the individual layers due to the arising current, which aligns the single Seebeck coefficients. When $S_s > S_f$, however, S_t can be larger than S_f , which can lead to misinterpretations when no analysis of the absolute value of ε_σ is performed beforehand. In the usual case of equal surface dimensions of the film and substrate, ε_σ can be written as

$$\varepsilon_\sigma = \frac{\sigma_s d_s}{\sigma_f d_f} \quad (11)$$

and only depends on the ratio of the conductivities and the thicknesses. Figure 2a shows $S_t(\varepsilon_\sigma)$ for different combinations of the Seebeck coefficient of the film $S_f = \{-50 \mu\text{V/K}, +50 \mu\text{V/K}\}$ and the substrate $S_s = \{-500 \mu\text{V/K}, -1000 \mu\text{V/K}\}$. Here, the values and signs are arbitrarily chosen and the influence of the substrate would be similar for positive Seebeck coefficients.

Since the thermoelectric properties depend on the film as well as the substrate, both need to be considered when calculating the overall power factor $PF_t = S_t^2 \sigma_t$ of the system. In order to be able to compare the power factor of film-substrate systems with bulk materials, the total thickness ($d_t = d_f + d_s$) must be used to calculate the total electrical conductivity, as long as no better assumption about the penetration depth of the current into the substrate can be made. This means that the total conductivity (see Figure 2b) is given from Equation 3 as

$$\begin{aligned} \sigma_t(\varepsilon_\sigma) &= (1 + \varepsilon_\sigma) \sigma_f \frac{d_f}{d_t} \\ &= \frac{(1 + \varepsilon_\sigma) \sigma_s \sigma_f}{\sigma_s + \varepsilon_\sigma \sigma_f} \end{aligned} \quad (12)$$

with the limits

$$\sigma_t = \begin{cases} \sigma_f & \text{for } \varepsilon_\sigma = 0 \\ \sigma_s & \text{for } \varepsilon_\sigma \rightarrow \infty \end{cases}. \quad (13)$$

On the other hand, if only the thickness of the film is used for calculating the electrical conductivity from the measured resistance ($d_t = d_f$), as is usually done, one

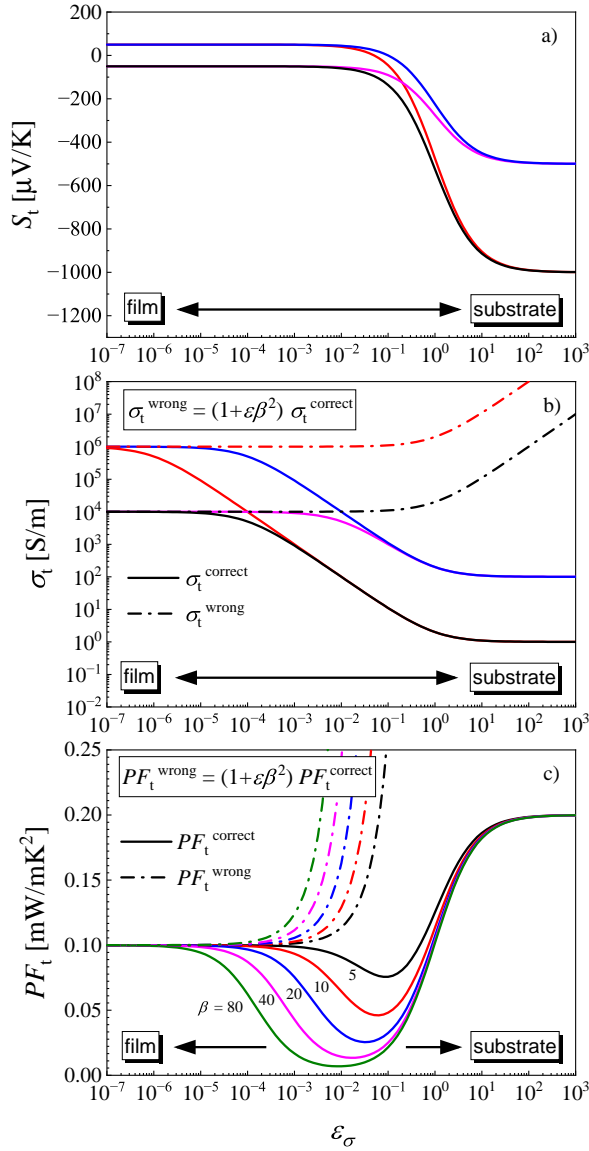


Figure 2: Calculated total a) Seebeck coefficient S_t , b) electrical conductivity σ_t and c) power factor PF_t of a film-substrate system with various thermoelectric properties, calculated from the equations derived in the text. The dashed-dotted lines show the wrong conductivity and power factor obtained by using the thickness of the film to calculate the total conductivity from the measured resistance. The power factor is shown for different values of $\beta = \sqrt{\sigma_f/\sigma_s}$. The values approach those of the film and the substrate for $\varepsilon_\sigma = 0$ and $\varepsilon_\sigma \rightarrow \infty$, respectively.

obtains

$$\sigma_t^{\text{wrong}}(\varepsilon_\sigma) = \sigma_f(1 + \varepsilon_\sigma). \quad (14)$$

It can be seen that for Equation 14, the total conductivity diverges ($\sigma_t \rightarrow \infty$) if the thickness of the film approaches 0 ($\varepsilon_\sigma \rightarrow \infty$). Thus, Equation 14 is only a

good approximation for small values of ε_σ , when either the film is sufficiently thick or the resistivity of the substrate is appropriately large compared to the resistivity of the film, meaning that the substrate is absolutely insignificant for electrical transport. The reason for the divergence of conductivity as the thickness of the film approaches zero is relatively straightforward. The calculated conductivity of a single material, obtained from the measured conductance, remains constant regardless of its dimensions. However, in the case of a two-layer setup where both layers make a significant contribution to conduction, the measured conductance does not decrease at the same rate as the thickness of one of the layers. As a result, as one layer becomes thinner, the error in the calculation becomes larger, ultimately leading to seemingly infinite conductivity when the thickness of the film becomes zero, since the conductance is still finite as current is still passing through the other layer.

Using Equation 9 and Equation 12, a more robust and general expression for the power factor of film-substrate systems can be derived (see Figure 2c):

$$PF_t(\varepsilon_\sigma) = \frac{S_f^2 + 2\varepsilon_\sigma S_f S_s + \varepsilon_\sigma^2 S_s^2}{(\sigma_s + \varepsilon_\sigma \sigma_f)(1 + \varepsilon_\sigma)} \sigma_s \sigma_f, \quad (15)$$

with the limits

$$PF_t = \begin{cases} S_f^2 \sigma_f = PF_f & \text{for } \varepsilon_\sigma = 0 \\ S_s^2 \sigma_s = PF_s & \text{for } \varepsilon_\sigma \rightarrow \infty \end{cases}. \quad (16)$$

PF_f and PF_s are the power factors of the film and the substrate, respectively. Equation 15 can also be rewritten in terms of the individual power factors $PF_{f,s}$:

$$PF_t(\varepsilon_\sigma) = \frac{(\sqrt{PF_f} + \varepsilon_\sigma \beta \sqrt{PF_s})^2}{(1 + \varepsilon_\sigma \beta^2)(1 + \varepsilon_\sigma)}, \quad (17)$$

with $\beta = \sqrt{\sigma_f/\sigma_s}$ being a material-dependent parameter. Notably, for $0 < \varepsilon_\sigma < \infty$ the total power factor is *always smaller* than the larger power factor of the two single materials (see Figure 2c). This shows that combining the Seebeck coefficient and electrical conductivity of the film and the substrate can never improve the total thermoelectric power factor, but only deteriorate it.

On the other hand, wrongly neglecting the current passing through the substrate and hence using Equation 14 leads to a total power factor of

$$PF_t^{\text{wrong}}(\varepsilon_\sigma) = \frac{(\sqrt{PF_f} + \varepsilon_\sigma \beta \sqrt{PF_s})^2}{1 + \varepsilon_\sigma}, \quad (18)$$

which *always* will result in power factors *larger* than that of the film alone for $0 < \varepsilon_\sigma < \infty$.

It is worth pointing out that this model, as it currently stands, is only quantitatively applicable to thick films. For thinner films, though the influence of the substrate increases even further, the impact of interface layers can modify the overall behavior significantly. Thus, the de-

rived equations can not be used to accurately calculate the total performance without taking this into consideration.

The thermal conductivity can be measured without a distorting influence of the substrate using the 3ω method [26]. Furthermore, the influence of the substrate to the total thermal conductance is usually treated with more care due to the high thermal conductivity of many commonly used substrates like Si, MgO or SrTiO₃. Thus, the thermal conductivity is less prone to misinterpretation. Because of the similarity between thermal and electrical conduction, the derivation of the total thermal conductivity is equal to the electrical conductivity. Based on Equation 12, the thermal conductivity of the simple system of non-interacting film and substrate is

$$\lambda_t(\varepsilon_\lambda) = \frac{(1 + \varepsilon_\lambda) \lambda_s \lambda_f}{\lambda_s + \varepsilon_\lambda \lambda_f}, \quad (19)$$

with λ_f and λ_s being the thermal conductivity of the film and the substrate, respectively, and

$$\varepsilon_\lambda = \frac{\lambda_s d_s}{\lambda_f d_f}, \quad (20)$$

denoting the contribution of the substrate to the thermal conduction. Once more, the total thermal conductivity has the limits

$$\lambda_t = \begin{cases} \lambda_f & \text{for } \varepsilon_\lambda = 0 \\ \lambda_s & \text{for } \varepsilon_\lambda \rightarrow \infty \end{cases} \quad (21)$$

and lies between the individual thermal conductivities for all other values.

Combining Equation 15 and Equation 19, the total figure of merit zT_t of the film-substrate system can be written as

$$zT_t = \frac{PF_t}{\lambda_t} T = \frac{(\sqrt{zT_f} + \sqrt{\varepsilon_\sigma \varepsilon_\lambda} \sqrt{zT_s})^2}{(1 + \varepsilon_\sigma)(1 + \varepsilon_\lambda)}, \quad (22)$$

which can only have values between zT_f and zT_s but never exceed the performance of the better layer. If, on the other hand, zT_t is calculated from the thermal conductivity of the film λ_f and the wrong power factor from Equation 18, neglecting the influence of the substrate to the electrical conduction, the overestimation is similar to the power factor shown in Figure 2c and will *always* lead to $zT_t > zT_f$.

This clearly shows that despite an increased Seebeck coefficient or electrical conductivity due to the contribution of the substrate may look beneficial, the thermoelectric performance can never be enhanced solely by the combination of the individual properties. This of course is only apparent if the influence of the substrate is considered when calculating the electrical conductivity. Otherwise, the power factor and figure of merit can reach wrong values far beyond that of the film.

While these results were derived for a film-substrate

system, it is valid for any two-layer and multi-layer system in general, since no specific assumptions about the layers were made. This means that a set of parallel layers will always have worse thermoelectric properties than the best performing layer. However, we emphasize that this does not exclude the possibility of an enhancement of the thermoelectric film performance with respect to the bulk material.

III. COMPARISON WITH EXPERIMENTAL DATA

To validate our derived formulas, we compare Equation 9 with experimental data from literature, where an influence of a conductive substrate on the overall properties is present. Figure 3a shows the thickness dependence of the Seebeck coefficient of a metallic Cu_{0.38}Ni_{0.62} film on a Si substrate [27] and a Ca₃Co₄O₉ film on a SrTiO₃ substrate [16]. The steadily increasing effect of the substrate with decreasing film thickness is clearly visible for films below 100 nm. Furthermore, plotting the data versus ε_σ , similar to Figure 2a, reveals remarkable agreement of the measured data with the trend predicted from our simple model, as shown in Figure 3b. The solid lines show the calculated S vs ε_σ evaluation in this system using Equation 9 without any free parameters. While the experimental data of the Cu-Ni films on Si follow our model curve extremely well, the absolute Seebeck coefficients of the Ca₃Co₄O₉ films on SrTiO₃ are larger than our predictions. This is most likely ascribed to two main issues, as indicated by the authors of Ref. [16] themselves: i) the presence of a potential interface layer, which could be considered using Equation 8 and ii) the very volatile incorporation of oxygen into SrTiO₃, having a drastic influence on the resistances. In fact, a correction of the ratio of the resistances, R_f/R_s , by a factor 5 to 10 leads to a significant improvement of the agreement between the second set of experimental data and our theory.

IV. CRITERION FOR THE SUBSTRATE INFLUENCE

After clarifying that the substrate can have a detrimental effect on the overall power factor and figure of merit compared to the properties of the film, we investigate the size of the measurement error when determining the thermoelectric properties of such systems. Since the thermal conductivity of the film can be measured separately and without contributions of the substrate, a potential error of the thermal conductivity is not considered here.

The deviation of the measured Seebeck coefficient from that of the film depends on both the ratio of the individual Seebeck coefficients and the value of ε_σ . While the former cannot be controlled, the latter can be altered by varying the thickness of the film and/or the substrate.

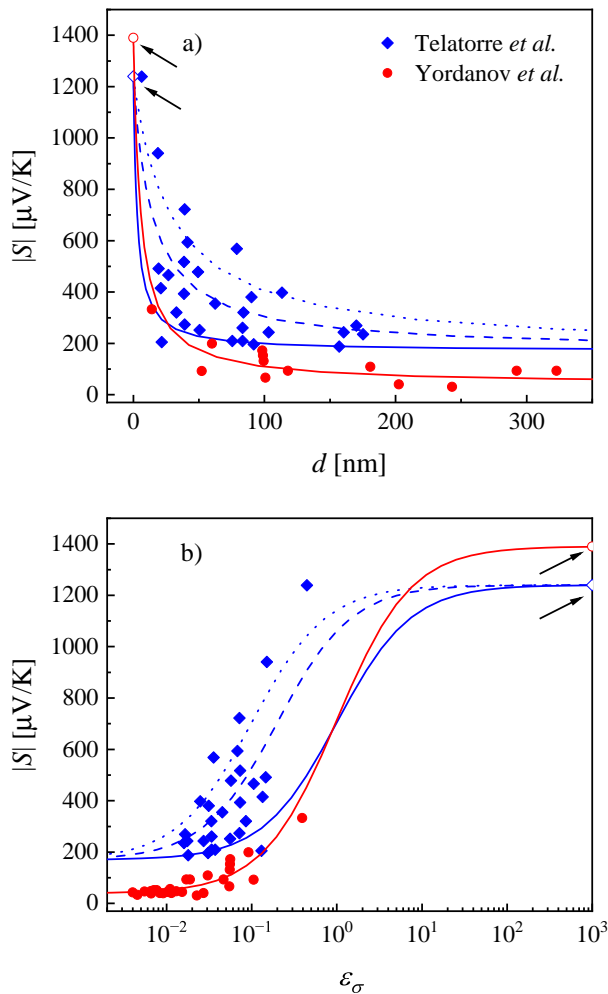


Figure 3: Seebeck coefficient of $\text{Cu}_{0.38}\text{Ni}_{0.62}$ films on Si [27] and $\text{Ca}_3\text{Co}_4\text{O}_9$ films on SrTiO_3 [16] in dependence of the thickness of the film (a) and the value of ε (b).

The solid lines show the total Seebeck coefficient calculated from Equation 9, whereas the dashed and dotted lines are based on the assumption that R_f/R_s is 5 times and 10 times larger, respectively. The Seebeck coefficient of the pristine substrates is shown by unfilled symbols and indicated by arrows. The values of the individual Seebeck coefficients, resistivities and thicknesses were taken from the respective literature.

Using Equation 9, the relative error δ_S can be written as

$$\delta_S = \frac{S_t - S_f}{S_f} = \frac{\varepsilon_\sigma}{1 + \varepsilon_\sigma} \left(\frac{S_s}{S_f} - 1 \right). \quad (23)$$

Table I shows the threshold values of ε_σ if the relative error of the Seebeck coefficient should not exceed δ_S .

Regarding the conductivity, the calculated value will be higher than the conductivity of the film in case of a contributing substrate. This problem can be circumvented by using Equation 12, which accounts for the total

	S_s/S_f		
	2	10	100
δ_S	$1.1 \cdot 10^{-1}$	$1.1 \cdot 10^{-2}$	$1.0 \cdot 10^{-3}$
0.05	$5.3 \cdot 10^{-2}$	$5.6 \cdot 10^{-3}$	$5.1 \cdot 10^{-4}$
0.01	$1.0 \cdot 10^{-2}$	$1.1 \cdot 10^{-3}$	$1.0 \cdot 10^{-4}$

Table I: Approximated threshold values of ε_σ in dependence of the desired upper limit of the relative error $\delta_S = (S_t - S_f)/S_f$ for various ratios of the individual Seebeck coefficients of substrate and film.

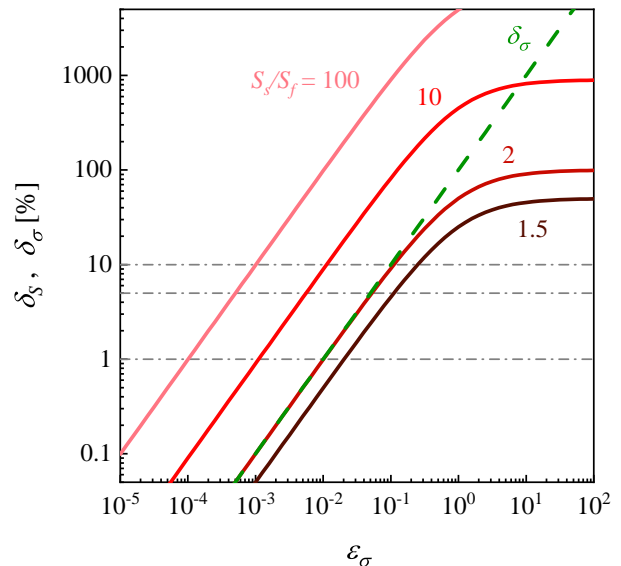


Figure 4: Relative error of the Seebeck coefficient for various ratios of the individual Seebeck coefficients of substrate S_s and film S_f (red solid lines) and relative error of the electrical conductivity (green dashed line) in dependence of the weighting parameter ε_σ . The gray dash-dotted lines mark relative errors of 1%, 5% and 10%.

thickness. It is, however, appropriate to use Equation 14 if the error

$$\delta_\sigma = \frac{\sigma_t - \sigma_f}{\sigma_f} = \varepsilon_\sigma. \quad (24)$$

is considered. The visualization of Equation 23 and Equation 24 is shown in Figure 4. For $S_s/S_f > 2$ the error of the Seebeck coefficient is larger than that of the conductivity in the region of interest. Thus, when evaluating the threshold of ε_σ the use of Equation 23 or Table I is sufficient.

Apart from determining the value of ε_σ , the process can be abbreviated by depositing the film on a well-known insulating material such as glass [14, 18, 28–33], MgO [16, 34–39], ZrO_2 [40–43] and plastic [44–51], which is indeed very common. On the other hand, reported results on semiconducting substrates should be interpreted

with additional caution as their influence can not be ruled out completely despite having a seemingly high resistivity [16, 18, 22, 29, 52–60].

V. CONCLUSION

Summarizing, we derived a set of formulas to describe the interplay of multiple electrically and thermally connected layers to the total thermoelectric performance in dependence of unique weighting parameters ε_σ and ε_λ , starting from a simple equivalent electric circuit. The results obtained confirm previous results that the overall thermoelectric performance of the entire composite, consisting *e.g.* of the substrate, an interface layer and the thermoelectric thin film is below that of the best performing layer. We further illustrated that the contribution of the substrate can lead to wrongly interpreted results if not considered in the analysis of the performance of a film.

Before choosing a substrate material for thermoelectric thin-film deposition, its influence on the power factor has to be clarified. We argue that this is best done by following three crucial steps:

- 1) Estimating the electrical conductivity and Seebeck coefficient of both the film and the substrate.
- 2) Calculating the threshold value of ε_σ based on the desired limit of the error $\delta_{s,\sigma}$.
- 3) Choosing the thickness of the film (and the substrate) according to Equation 11 or selecting a different substrate with a sufficiently low electrical conductivity.

Apart from the influence on the power factor, the plausibility of a low thermal conductivity of the film in the presence of a highly heat-conducting substrate needs to be questioned, as the overall figure of merit of the system is deteriorated. When comparing the performance of a material system, it is important to consider the total thickness of the system, including any non-contributing substrates. This will ensure an accurate calculation of the total power factor or figure of merit, taking into account the additional space acquired by the substrate.

ACKNOWLEDGMENTS

Financial support for the research in this paper was granted by the Japan Science and Technology Agency (JST) programs MIRAI, JPMJMI19A1.

-
- [1] C. Forman, I. K. Muritala, R. Pardemann, and B. Meyer, Estimating the global waste heat potential, *Renewable and Sustainable Energy Reviews* **57**, 1568 (2016).
 - [2] I. Petsagkourakis, K. Tybrandt, X. Crispin, I. Ohkubo, N. Satoh, and T. Mori, Thermoelectric materials and applications for energy harvesting power generation, *Science and technology of advanced materials* **19**, 836 (2018).
 - [3] M. Burton, G. Howells, J. Atoyo, and M. Carnie, Printed thermoelectrics, *Advanced Materials* , 2108183 (2022).
 - [4] L. E. Bell, Cooling, heating, generating power, and recovering waste heat with thermoelectric systems, *Science* **321**, 1457 (2008).
 - [5] Y. Furuta, K. Kato, T. Miyawaki, H. Asano, and T. Takeuchi, Fe₂VAl-based thermoelectric thin films prepared by a sputtering technique, *Journal of electronic materials* **43**, 2157 (2014).
 - [6] S. Hiroi, M. Mikami, and T. Takeuchi, Thermoelectric properties of Fe₂VAl-based thin-films deposited at high temperature, *Materials transactions* **57**, 1628 (2016).
 - [7] S. Hiroi, M. Mikami, K. Kitahara, and T. Takeuchi, Thickness dependence of thermal conductivity and electron transport properties of Fe₂VAl thin-films prepared by RF sputtering technique, *International Journal of Nanotechnology* **13**, 881 (2016).
 - [8] S. Yamada, K. Kudo, R. Okuhata, J. Chikada, Y. Nakamura, and K. Hamaya, Low thermal conductivity of thermoelectric Fe₂VAl films, *Applied Physics Express* **10**, 115802 (2017).
 - [9] S. Hiroi, S. Nishino, S. Choi, O. Seo, J. Kim, Y. Chen, C. Song, A. Tayal, O. Sakata, and T. Takeuchi, Phonon scattering at the interfaces of epitaxially grown Fe₂VAl/W and Fe₂VAl/Mo superlattices, *Journal of Applied Physics* **125**, 225101 (2019).
 - [10] K. Kudo, S. Yamada, J. Chikada, Y. Shimanuki, T. Ishibe, S. Abo, H. Miyazaki, Y. Nishino, Y. Nakamura, and K. Hamaya, Significant reduction in the thermal conductivity of Si-substituted Fe₂VAl epilayers, *Physical Review B* **99**, 054201 (2019).
 - [11] B. Hinterleitner, I. Knapp, M. Poneder, Y. Shi, H. Müller, G. Eguchi, C. Eisenmenger-Sittner, M. Stöger-Pollach, Y. Kakefuda, N. Kawamoto, *et al.*, Thermoelectric performance of a metastable thin-film heusler alloy, *Nature* **576**, 85 (2019).
 - [12] S. Choi, S. Hiroi, M. Inukai, S. Nishino, R. Sobota, D. Byeon, M. Mikami, E. Minamitani, M. Matsunami, and T. Takeuchi, Crossover in periodic length dependence of thermal conductivity in 5d element substituted Fe₂VAl-based superlattices, *Physical Review B* **102**, 104301 (2020).
 - [13] Y. Shimanuki, K. Kudo, T. Ishibe, A. Masago, S. Yamada, Y. Nakamura, and K. Hamaya, Thermoelectric properties of single-phase full-heusler alloy Fe₂TiSi films with D₀₃-type disordering, *Journal of Applied Physics* **127**, 055106 (2020).
 - [14] W. Gao, Z. Liu, T. Baba, Q. Guo, D.-M. Tang, N. Kawamoto, E. Bauer, N. Tsujii, and T. Mori, Significant off-stoichiometry effect leading to the n-type conduction and ferromagnetic properties in titanium doped Fe₂VAl thin films, *Acta Materialia* **200**, 848 (2020).
 - [15] H. Pang, C. Bourgès, R. Jha, T. Baba, N. Sato, N. Kawamoto, T. Baba, N. Tsujii, and T. Mori, Revealing an elusive metastable wurtzite CuFeS₂ and the phase switching between wurtzite and chalcopyrite for thermoelectric thin films, *Acta Materialia* , 118090 (2022).

- [16] P. Yordanov, P. Wochner, S. Ibrahimkuty, C. Dietl, F. Wrobel, R. Felici, G. Gregori, J. Maier, B. Keimer, and H.-U. Habermeier, Perovskite substrates boost the thermopower of cobaltate thin films at high temperatures, *Applied Physics Letters* **110**, 253101 (2017).
- [17] S. Shimizu, J. Shiogai, N. Takemori, S. Sakai, H. Ikeda, R. Arita, T. Nojima, A. Tsukazaki, and Y. Iwasa, Giant thermoelectric power factor in ultrathin FeSe superconductor, *Nature communications* **10**, 1 (2019).
- [18] J. Zhang, W. Song, X. Ge, Z. Luo, and S. Yue, Boosted thermoelectric properties of molybdenum oxide thin films deposited on Si substrates, *Modern Physics Letters B* **33**, 1950016 (2019).
- [19] D. Byeon, R. Sobota, K. Delime-Codrin, S. Choi, K. Hirata, M. Adachi, M. Kiyama, T. Matsuura, Y. Yamamoto, M. Matsunami, *et al.*, Discovery of colossal seebeck effect in metallic Cu₂Se, *Nature communications* **10**, 1 (2019).
- [20] D. Byeon, R. Sobota, S. Singh, S. Ghodke, S. Choi, N. Kubo, M. Adachi, Y. Yamamoto, M. Matsunami, and T. Takeuchi, Long-term stability of the colossal seebeck effect in metallic Cu₂Se, *Journal of Electronic Materials* , 1 (2020).
- [21] G. Kim, D. Byeon, S. Singh, K. Hirata, S. Choi, M. Matsunami, and T. Takeuchi, Mixed-phase effect of a high seebeck coefficient and low electrical resistivity in Ag₂S, *Journal of Physics D: Applied Physics* **54**, 115503 (2021).
- [22] X. Ge, H. Zhu, and S. Yue, Optimization of large power factor in molybdenum oxide thin films deposited on Si substrate, *Modern Physics Letters B* , 2050200 (2020).
- [23] D. J. Bergman and O. Levy, Thermoelectric properties of a composite medium, *Journal of Applied Physics* **70**, 6821 (1991).
- [24] D. J. Bergman and L. G. Fel, Enhancement of thermoelectric power factor in composite thermoelectrics, *Journal of Applied physics* **85**, 8205 (1999).
- [25] J. Alvarez-Quintana, Impact of the substrate on the efficiency of thin film thermoelectric technology, *Applied Thermal Engineering* **84**, 206 (2015).
- [26] C. Dames, Measuring the thermal conductivity of thin films: 3 omega and related electrothermal methods, *Annual Review of Heat Transfer* **16** (2013).
- [27] R. Delatorre, M. Sartorelli, A. Schervenski, A. Pasa, and S. Güths, Thermoelectric properties of electrodeposited CuNi alloys on Si, *Journal of applied physics* **93**, 6154 (2003).
- [28] F. Qiu, W. Shin, M. Matsumiya, N. Izu, I. Matsubara, and N. Murayama, Miniaturization of thermoelectric hydrogen sensor prepared on glass substrate with low-temperature crystallized SiGe film, *Sensors and Actuators B: Chemical* **103**, 252 (2004).
- [29] Y. Hu, E. Sutter, W. Si, and Q. Li, Thermoelectric properties and microstructure of c-axis-oriented Ca₃Co₄O₉ thin films on glass substrates, *Applied Physics Letters* **87**, 171912 (2005).
- [30] X. Zhang, Z. Pei, J. Gong, and C. Sun, Investigation on the electrical properties and inhomogeneous distribution of ZnO: Al thin films prepared by dc magnetron sputtering at low deposition temperature, *Journal of applied physics* **101**, 014910 (2007).
- [31] Z. Yu, X. Wang, Y. Du, S. Aminorroaya-Yamni, C. Zhang, K. Chuang, and S. Li, Fabrication and characterization of textured Bi₂Te₃ thermoelectric thin films prepared on glass substrates at room temperature using pulsed laser deposition, *Journal of crystal growth* **362**, 247 (2013).
- [32] S. Mortazavinatanzi, M. Mirhosseini, L. Song, B. B. Iversen, L. Rosendahl, and A. Rezaia, Zinc antimonide thin film based flexible thermoelectric module, *Materials Letters* **280**, 128582 (2020).
- [33] N. A. Khan, M. A. Alnuwaiser, M. R. Javed, S. Ikram, A. Ali, M. Y. Ali, M. Amami, M. A. Nawaz, K. Javaid, M. S. Hussain, *et al.*, Effect of Sn concentration on the structural, morphological and thermoelectric transport properties of zinc stannates thin films, *Ceramics International* **48**, 35237 (2022).
- [34] M. Matsumiya, F. Qiu, W. Shin, N. Izu, N. Murayama, and S. Kanzaki, Thin-film Li-doped NiO for thermoelectric hydrogen gas sensor, *Thin Solid Films* **419**, 213 (2002).
- [35] T. Jaeger, C. Mix, M. Schwall, X. Kozina, J. Barth, B. Balke, M. Finsterbusch, Y. U. Idzerda, C. Felser, and G. Jakob, Epitaxial growth and thermoelectric properties of TiNiSn and Zr_{0.5}Hf_{0.5}NiSn thin films, *Thin Solid Films* **520**, 1010 (2011).
- [36] P. V. Burmistrova, J. Maassen, T. Favaloro, B. Saha, S. Salamat, Y. Rui Koh, M. S. Lundstrom, A. Shakouri, and T. D. Sands, Thermoelectric properties of epitaxial ScN films deposited by reactive magnetron sputtering onto MgO (001) substrates, *Journal of Applied Physics* **113**, 153704 (2013).
- [37] A. T. Duong, S. Rhim, Y. Shin, V. Q. Nguyen, and S. Cho, Magneto-transport and thermoelectric properties of epitaxial FeSb₂ thin film on MgO substrate, *Applied Physics Letters* **106**, 032106 (2015).
- [38] P. V. Burmistrova, D. N. Zakharov, T. Favaloro, A. Mohammed, E. A. Stach, A. Shakouri, and T. D. Sands, Effect of deposition pressure on the microstructure and thermoelectric properties of epitaxial ScN (001) thin films sputtered onto MgO (001) substrates, *Journal of Materials Research* **30**, 626 (2015).
- [39] Y. Kurosaki, S. Yabuuchi, A. Nishide, N. Fukatani, and J. Hayakawa, Thermoelectric properties of composition-controlled Fe₂TiSi-based full-Heusler thin films, *Applied Physics Express* **15**, 085502 (2022).
- [40] A. Matsumoto, M. Mikami, K. Kobayashi, K. Ozaki, and T. Nishio, Preparation of Fe₂VAl thermoelectric module by RF sputtering, in *Materials science forum*, Vol. 539 (Trans Tech Publ, 2007) pp. 3285–3289.
- [41] M. Mikami, T. Kamiya, and K. Kobayashi, Microstructure and thermoelectric properties of Heusler Fe₂VAl thin-films, *Thin Solid Films* **518**, 2796 (2010).
- [42] J. Buršík, M. Soroka, K. Knížek, J. Hirschner, P. Levinský, and J. Hejtmánek, Oriented thin films of Na_{0.6}CoO₂ and Ca₃Co₄O₉ deposited by spin-coating method on polycrystalline substrate, *Thin Solid Films* **603**, 400 (2016).
- [43] A. Pérez-Rivero, M. Cabero, M. Varela, R. Ramírez-Jiménez, F. Mompean, J. Santamaría, J. Martínez, and C. Prieto, Thermoelectric functionality of Ca₃Co₄O₉ epitaxial thin films on yttria-stabilized zirconia crystalline substrate, *Journal of Alloys and Compounds* **710**, 151 (2017).
- [44] L. Goncalves, C. Couto, P. Alpuim, A. G. Rolo, F. Völklein, and J. Correia, Optimization of thermoelectric properties on Bi₂Te₃ thin films deposited by thermal co-evaporation, *Thin Solid Films* **518**, 2816 (2010).

- [45] M. Hokazono, H. Anno, and N. Toshima, Thermoelectric properties and thermal stability of PEDOT: PSS films on a polyimide substrate and application in flexible energy conversion devices, *Journal of Electronic Materials* **43**, 2196 (2014).
- [46] C. T. Hong, Y. H. Kang, J. Ryu, S. Y. Cho, and K.-S. Jang, Spray-printed CNT/P3HT organic thermoelectric films and power generators, *Journal of Materials Chemistry A* **3**, 21428 (2015).
- [47] T. Varghese, C. Hollar, J. Richardson, N. Kempf, C. Han, P. Gamarrachchi, D. Estrada, R. J. Mehta, and Y. Zhang, High-performance and flexible thermoelectric films by screen printing solution-processed nanoplate crystals, *Scientific reports* **6**, 1 (2016).
- [48] Z. Lin, C. Hollar, J. S. Kang, A. Yin, Y. Wang, H.-Y. Shiu, Y. Huang, Y. Hu, Y. Zhang, and X. Duan, A solution processable high-performance thermoelectric copper selenide thin film, *Advanced Materials* **29**, 1606662 (2017).
- [49] S. Yang, K. Cho, J. Yun, J. Choi, and S. Kim, Thermoelectric characteristics of γ -Ag₂Te nanoparticle thin films on flexible substrates, *Thin Solid Films* **641**, 65 (2017).
- [50] K. Kusano, A. Yamamoto, M. Nakata, T. Suemasu, and K. Toko, Thermoelectric inorganic SiGe film synthesized on flexible plastic substrate, *ACS Applied Energy Materials* **1**, 5280 (2018).
- [51] W. Ren, Y. Sun, D. Zhao, A. Aili, S. Zhang, C. Shi, J. Zhang, H. Geng, J. Zhang, L. Zhang, *et al.*, High-performance wearable thermoelectric generator with self-healing, recycling, and lego-like reconfiguring capabilities, *Science advances* **7**, eabe0586 (2021).
- [52] M. Takashiri, T. Borca-Tasciuc, A. Jacquot, K. Miyazaki, and G. Chen, Structure and thermoelectric properties of boron doped nanocrystalline Si_{0.8}Ge_{0.2} thin film, *Journal of applied physics* **100**, 054315 (2006).
- [53] M. Aguirre, S. Canulescu, R. Robert, N. Homazava, D. Logvinovich, L. Bocher, T. Lippert, M. Döbeli, and A. Weidenkaff, Structure, microstructure, and high-temperature transport properties of La_{1-x}Ca_xMnO_{3- δ} thin films and polycrystalline bulk materials, *Journal of Applied Physics* **103**, 013703 (2008).
- [54] H. B. Lee, J. H. We, H. J. Yang, K. Kim, K. C. Choi, and B. J. Cho, Thermoelectric properties of screen-printed ZnSb film, *Thin Solid Films* **519**, 5441 (2011).
- [55] P. Mele, S. Saini, H. Honda, K. Matsumoto, K. Miyazaki, H. Hagino, and A. Ichinose, Effect of substrate on thermoelectric properties of Al-doped ZnO thin films, *Applied Physics Letters* **102**, 253903 (2013).
- [56] A. Nozariasbmarz, A. T. Rad, Z. Zamanipour, J. S. Krasinski, L. Tayebi, and D. Vashaee, Enhancement of thermoelectric power factor of silicon germanium films grown by electrophoresis deposition, *Scripta Materialia* **69**, 549 (2013).
- [57] J. Jacob, R. Wahid, A. Ali, R. Zahra, S. Ikram, N. Amin, A. Ashfa, U. Rehman, S. Hussain, D. S. Al-Othmany, *et al.*, Growth of Cu₂InO₄ thin films on Si substrate by thermal evaporation technique and enhancement of thermoelectric properties by post-growth annealing, *Physica B: Condensed Matter* **562**, 59 (2019).
- [58] U. Rehman, J. Jacob, K. Mahmood, A. Ali, A. Ashfaq, N. Amin, S. Ikram, W. Ahmad, and S. Hussain, Direct growth of ZnSnO nano-wires by thermal evaporation technique for thermoelectric applications, *Physica B: Condensed Matter* **570**, 232 (2019).
- [59] U. Rehman, K. Mahmood, A. Ali, A. Ashfaq, A. Rehman, M. A. un Nabi, M. I. Arshad, N. Amin, S. Ikram, and S. Hussain, Optimizing the electrical transport properties of ZnSnO thin films by post growth annealing in air, *Optik* **204**, 164148 (2020).
- [60] A. Grieser, T. Kraus, O. Klein, and H. Karl, Low-resistance electrical contact between epitaxially grown thermoelectric oxide material (Ca₂CoO₃)_{0.62}CoO₂ and iridium, *Thin Solid Films* **717**, 138420 (2021).